

Plasma-Treated Ce/TiO₂-Palygorskite Catalyst for the NH₃-SCR of NO_x

^{1,2}Kaige Chen, ¹Ruoyu Chen, ²Zhe Tang, ²Hui Cang*, ²Qi Xu**

¹School of Petrochemical Engineering, Changzhou University, Changzhou 213164, Jiangsu Province, China.

²Yancheng Institute of Technology, Yancheng 224051, Jiangsu Province, China.

canghui_ycit@126.com*; xqsteve@ycit.cn**

(Received on 21st April 2017, accepted in revised form 4th July 2018)

Summary: Ce/TiO₂-Palygorskite ternary composites were fabricated as an efficient catalyst for medium and low temperature NH₃-SCR reaction and the optimal mass proportion (Ti:Pal=1:3) of this catalyst was confirmed by the catalytic performance test, in order to improve the surface dispersion, which needed to be further disposed by the Non-thermal plasma, after that, it was activated by thermal treatment at 400°C for 4 h. Based on the results obtained by XRD, FE-SEM, TEM, NH₃-TPD, UV-vis (DRS), XPS, the treatment of plasma was much essential for the transformation from Ce⁴⁺ to Ce³⁺ on the surface of Ce/TiO₂-palygorskite, to increase surface chemisorbed oxygen, and the improved dispersion, which were highly favorable for denitration. At about 350 °C, the best NO conversion was respectively 90.59 % and 96.78 % for the untreated and treated catalysts, the latter possessed higher N₂ selectivity. Besides, according to the research results on alkali metals poisoning resistance of these catalysts, it was discovered, the treated-catalyst poisoned by sodium salt had the best resistance performance, which might be related with the modification of the Non-thermal plasma, leading to more dispersed surface acid sites, to get more active sites, meanwhile, the toxicity of K was stronger than Na.

Key words: NH₃-SCR, Plasma, Chemisorbed oxygen, Denitration, Alkali metals.

Introduction

Regarded as non-renewable energy, fossil fuels had ever been widely used among the power plants, which led to the generation of various atmospheric pollutants, especially nitrogen oxides (NO_x, x=1, 2), however, the amount of NO₂ was less than one-tenth of NO in the total nitrogen oxide emission [1], which contributed to a series of environmental issues including acid rain, ozone depletion, greenhouse effect and Particulate Matter_{2.5}. Among the various technologies developed to reduce NO, the NH₃-SCR was the most widely used technology for removing NO from stationary sources. An efficient catalyst played a key role for this technology under actual working conditions, including coal-fired power plants and biomass combustion equipment. Currently, Ti-based catalysts such as V₂O₅-WO₃/TiO₂, V₂O₅-MoO₃/TiO₂ are of great interest for the commercial manufacturers, although, these catalysts have many advantages including excellent catalytic activity, good sulfur resistance and interaction with active components, however, there are still some defects, such as high starting temperature, narrow active temperature, falling N₂ selectivity at high temperature and poor thermal stability[2]. Withal, substantial work had been done to improve those properties of Ti-based catalysts via increasing of Lewis acid, expansion of active temperature window, control of initial structure sintering [3-6]. In addition, surface stabilizers (SiO₂, Al₂O₃) were employed to improve the performance of Ti-based catalysts, it is well known that SiO₂ can

provide a large surface area for the loading of active components, and its silicon hydroxyl groups exhibit high thermal stability. Likewise, Al₂O₃ can be also incorporated with TiO₂ to prepare the composite carrier TiO₂-Al₂O₃, which is enriched in microporous structure, to make for the dispersion of various ingredients on the surface [7-8]. Zhao *et al* [9]. reported novel Ce/TiO₂-SiO₂ (Al₂O₃) catalysts respectively, the results indicated the addition of SiO₂ or Al₂O₃ could be conducive to the existence of Ce³⁺, to generate oxygen vacancies, which can increase the oxygen adsorption and is in favour of the conversion of NO to NO₂ [10].

Transition metals containing Fe, Cu and V had been investigated as promising active components for Ti-based catalysts in the NH₃-SCR system [11-13]. Moreover, Ce had also been reported extensively due to perfect oxygen storage capacity by the transformation between Ce⁴⁺ and Ce³⁺, in comparison with V, which was very nontoxic. Besides, in order to further broaden the superior performances over the catalyst among the application of NH₃-SCR reaction, many investigators also took great efforts on the modification of the catalysts, and once previous research showed that plasma treatment was an effective method to improve the dispersion of the active sites over the catalysts. Liu *et al.* [14] had reported that the particle size of PdO₂ over a plasma-treated sample was smaller than that in an untreated sample; hence the plasma-treated sample

*To whom all correspondence should be addressed.

was of both the high dispersion of Brønsted and Lewis acid sites. Moreover, Li *et al.* [15] also found that the metal dispersion could be increased by the NTP treatment, and thus resulting in higher NO_x storage. Tang *et al.* [16] investigated the effect of non-thermal treatment on the structural and morphological properties of the Mn-CoO_x catalyst.

In this work, palygorskite as base material was combined with certain amount of TiO_2 to prepare a novel composite carrier TiO_2 -palygorskite, followed by the dipping load of 10wt% Ce, to prepare a series of Ce/ TiO_2 -palygorskite catalysts, which were further treated by the Non-thermal Plasma (Ar). The effects of plasma treatment on surface dispersion and catalytic performance of the as-prepared catalysts were investigated systematically.

Experimental

Catalyst Preparation

5 ml Tetrabutyl titanate (TiO_2 , 1.18 g) was mixed with 8 ml anhydrous ethanol by vigorous stirring and then adding 6 drops of glacial acetic acid dropwise, to obtain solution, 16 ml anhydrous ethanol, 10 drops of deionized water and 2 drops of nitric acid were placed into other beak to form mixed solution, and then dropwise added in the solution with vigorous stirring at 40 °C. Afterwards, certain amount of Pal-purification was poured into the above mentioned solution and vigorously stirred for 1 h, which was then aged for 48 h. The resulting mixed solution was dried at 80 °C and subsequently calcined at 400 °C for 4 h, ground and sieved (50-60 mesh) to obtain the composite carrier TiO_2 -palygorskite (TiO_2/Pal (mass ratios) = 1:1, 1:2, 1:3, 1:4).

The support material of TiO_2 -palygorskite was impregnated with cerium nitrate solution, stirred for 2 h and aged for 48 h, dried at 80 °C and calcined at 400 °C for 4 h in static air. Finally, 10wt% Ce/ TiO_2 -palygorskite catalysts were prepared and denoted as Ce/ TiO_2 -Pal (x), where x corresponded to the mass ratio between TiO_2 and Pal.

Non-thermal Plasma Modification

Before calcination, the optimal catalyst sample was placed on a Pyrex plate ($d=10$ cm) under a glow discharge plasma system for plasma treatment. The entire disposal system consisted of a vacuum pump, Pyrex tube reactor, solid-state high-frequency power supply, and gas resource Argon (>99.99% in purity). The above-mentioned sample was treated on the glow discharge reactor at output powers of 100 W

for 30 min, and firstly, the Pyrex tube reactor was evacuated and then the argon was introduced, maintaining the internal pressure within 30–50 Pa. The sample treated by the non-thermal plasma, followed by calcination, was labeled as Ce/ TiO_2 -Pal (NTP) for testing. The specific treatment device is illustrated in Fig. 1a, and an image of the glow discharge with the power being treated was shown in Fig. 1b.

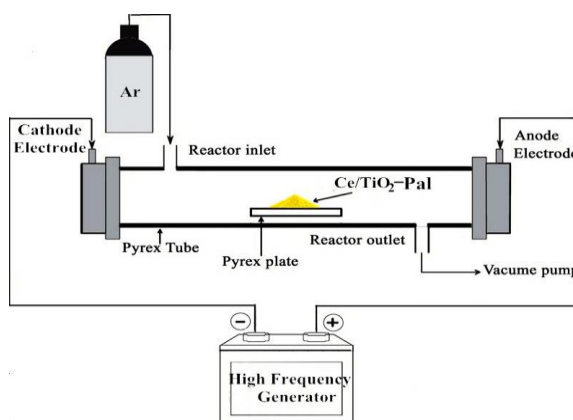


Fig. 1: (a). Schematic diagram of non-thermal plasma disposal device.



Fig. 1: b. Image of the glow discharge process.

Alkali Poisoning

K_2O and Na_2O poisoning experiments with the mass ratios ($\text{K}^+/\text{catalyst}=1\%$, $\text{Na}^+/\text{catalyst}=1.5\%$), were prepared by the impregnation method, with the nitrate solution. The mixture was mixed under stirring at room temperature for 1h continuously and dried at 105°C for 6h. Then the solid samples were

respectively calcined at 450°C for 4h in air, ground and sieved (50-60 mesh) to get the alkali poisoning catalysts.

Characterization of Catalysts

The crystalline structure of all catalysts was determined by XRD patterns, collected on a Rigaku D/Max2500PC diffractometer with Cu K α radiation ($\lambda = 0.15406$ nm) at 60 KV and 30 mA among a scan range of 0°–80° at 5°/min. The crystalline phases were identified by referring to the database of the International Center for Diffraction Data (ICDD). The UV-vis spectra were obtained in the diffuse reflectance mode using a Shimadzu UV-2600 spectrometer and BaSO₄ as a reference. The surface morphology of the samples was determined by scanning electron microscopy (SEM) and transmission electron microscopy (TEM). The distribution of acidic sites on the catalyst surface was investigated by NH₃-TPD with a fixed-bed quartz reactor and 100 mg of the sample at a gas flow rate of 30 mL/min. X-ray photoelectron spectroscopy (XPS) spectrums were obtained using a K-Al photoelectron spectrometer with standard Al K α radiation (1486.7 eV) at 350 W (XSAM800, Kratos Analytical, UK). The binding energies of the samples were calibrated using the adventitious C 1s peak at 284.6 eV; an instrument error of ± 0.1 eV was estimated during the experiment.

Activity Tests

The performance evaluation was carried out in a fixed-bed quartz reactor [17]. The apparatus included a simulated flue gas system, fixed-bed reactor, and gas analyzer system (MRU-VAR10 PLUS, Germany). The following simulated flue gas conditions were used: 3vol% O₂, 500 ppm NO, 500 ppm NH₃, and the balance gas N₂. The total gas flow was fixed at 500 mL/min. About 0.67 mL of the catalyst was packed in a quartz tube, corresponding to a gas hour space velocity (GHSV) of 45000 h⁻¹. The outlet NH₃ was tested by using an in situ sampling analysis system (XLZ-1090GXH, The Forest Science and Technology Development Co.,

Ltd., China). The NO removal efficiency and N₂ selectivity were determined by the following equations:

Results and Discussion

Characterization and Performance Analysis of Untreated Catalysts

From the Fig. 2, it could be illustrated for the XRD patterns of CeO₂/TiO₂-Pal, their crystalline phases were identified by comparison with ICDD files (anatase TiO₂, 21-1272; Palygorskite, 31-0783; cubic CeO₂, 34-0394). The typical diffraction peaks at $2\theta = 10\text{--}50^\circ$ were respectively corresponding to the primary diffraction of the (110) plane for Pal, the (101) plane for anatase TiO₂ and the (004) plane for cubic CeO₂. With the increasing relative content of Pal, the characteristic diffraction peaks of Pal and cubic CeO₂ were broadened, and the averaged crystalline size (D) [18] of anatase TiO₂ was determined according to the diffraction peak indexed to the crystal plane using the Scherrer equation (Klug and Alexander, 1974):

$$D = 0.89\lambda / (\beta \cos \theta)$$

where, λ is the wavelength of radiation, β is the corrected peak width at half-maximum intensity (FWHM in radians), and θ is half of the peak position. It could be seen that the crystalline size of anatase TiO₂ was decreased accordingly, which indicated that the addition of ATP was good for the dispersion of TiO₂ particles and active species Ce, inhibited the growth of grain size of anatase TiO₂. However, at the mass ratio of 1:4, the averaged crystalline size of TiO₂ was increased again and the diffraction peak of cubic CeO₂ became stronger, but the peak at $2\theta = 8.24^\circ$ for Pal was almost disappeared, which might be related with the reduction of TiO₂ particles, inducing the aggregation of some active species Ce on the surface of TiO₂, thus the optimal mass ratio of the composite carrier was of great importance. Table 1 displayed the crystalline size of anatase TiO₂ for different samples.

$$NO_{conversion} (\%) = \frac{[NO]_{in} - [NO]_{out}}{[NO]_{in}} \times 100\%$$

$$N_{2selectivity} (\%) = \frac{[NO]_{in} + [NH_3]_{in} - [NO]_{out} - [NH_3]_{out} - 2[NO_2]_{out}}{[NO]_{in} + [NH_3]_{in} - [NO]_{out} - [NH_3]_{out}} \times 100\%$$

Table-1: Surface area, Crystalline phase and crystalline sizes of various samples (Anatase TiO₂).

Sample	Crystal plane	2theta(°)	Intensity	FMWH(rad) ^a	D(nm) ^b	Surface area(m ² /g)
Ce/TiO ₂ :Pal(1:1)	101	25.34	100%	0.01416	10.1	113.3
Ce/TiO ₂ :Pal(1:2)	101	25.50	100%	0.01427	10.0	116.7
Ce/TiO ₂ :Pal(1:3)	101	25.34	100%	0.01535	9.20	129.5
Ce/TiO ₂ :Pal(1:4)	101	25.30	100%	0.01485	9.60	124.1
Ce/TiO ₂ :Pal(1:3)-NTP	101	25.40	100%	0.01603	8.81	143.2

^a Corrected peak width at half-maximum intensity ^b Crystallite size

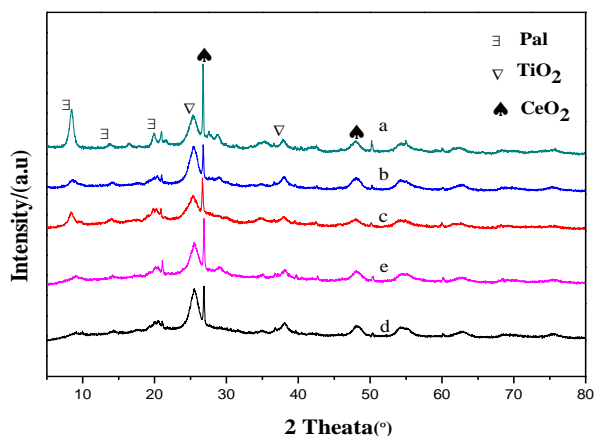


Fig. 2: XRD patterns of Ce/TiO₂-Pal catalysts: a, Ce/TiO₂-Pal (1:1); b, Ce/TiO₂-Pal (1:2); c, Ce/TiO₂-Pal (1:3); d, Ce/TiO₂-Pal (1:4); e, Ce/TiO₂-Pal (1:3)-NTP.

Fig.3a showed the UV-Vis diffuse reflectance spectra of different carriers, the absorption edge of Pal appeared at 248 nm, when loading with TiO₂, which had an obvious red shift, due to the charge transfer between the conduction band or the valence band of TiO₂ and Pal, it could be also seen that TiO₂/Pal (1:3) showed the largest red shift. Meanwhile, the addition of Ce resulted in further red shift, which might be beneficial to improving the redox properties of the catalysts [19], as shown in Fig.3b.

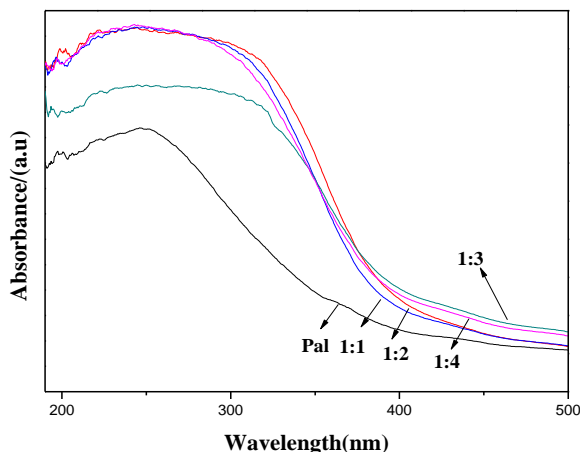


Fig. 3: a. UV-Vis DRS spectra of carriers.

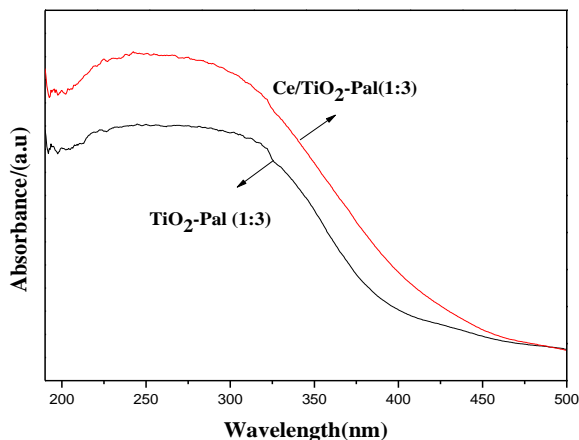


Fig. 3b: UV-Vis DRS spectra of carriers before and after the load of Ce.

NO conversion efficiency over various Ce/TiO₂-Pal catalysts at different temperatures was displayed in Fig.4. The Ce/TiO₂-Pal (1:3) catalyst exhibited the highest activity among the catalysts with different mass ratios of composite carrier, and its NO conversion reached by 90.59 % at about 350 °C, which was consistent with the results of XRD and UV-vis analysis. Notably, the activities of the cerium catalysts were higher in the temperature range of 250-450 °C. Therefore, the Ce/TiO₂-Pal (1:3) was further treated by the plasma, to improve its surface dispersion.

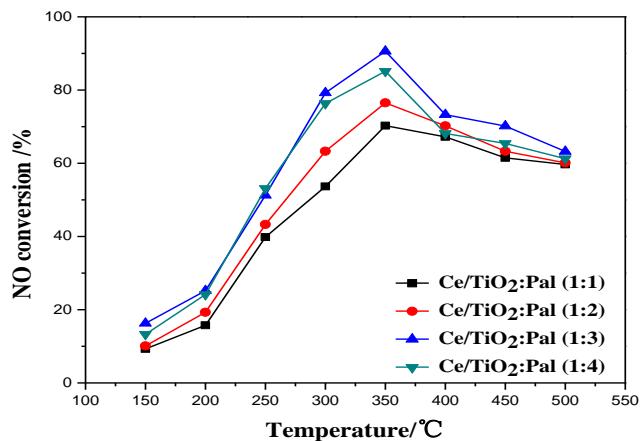


Fig. 4: NO conversion of Ce/TiO₂-Pal catalysts: TiO₂/Pal (1:1), TiO₂/Pal (1:2), TiO₂/Pal (1:3), TiO₂/pal (1:4).

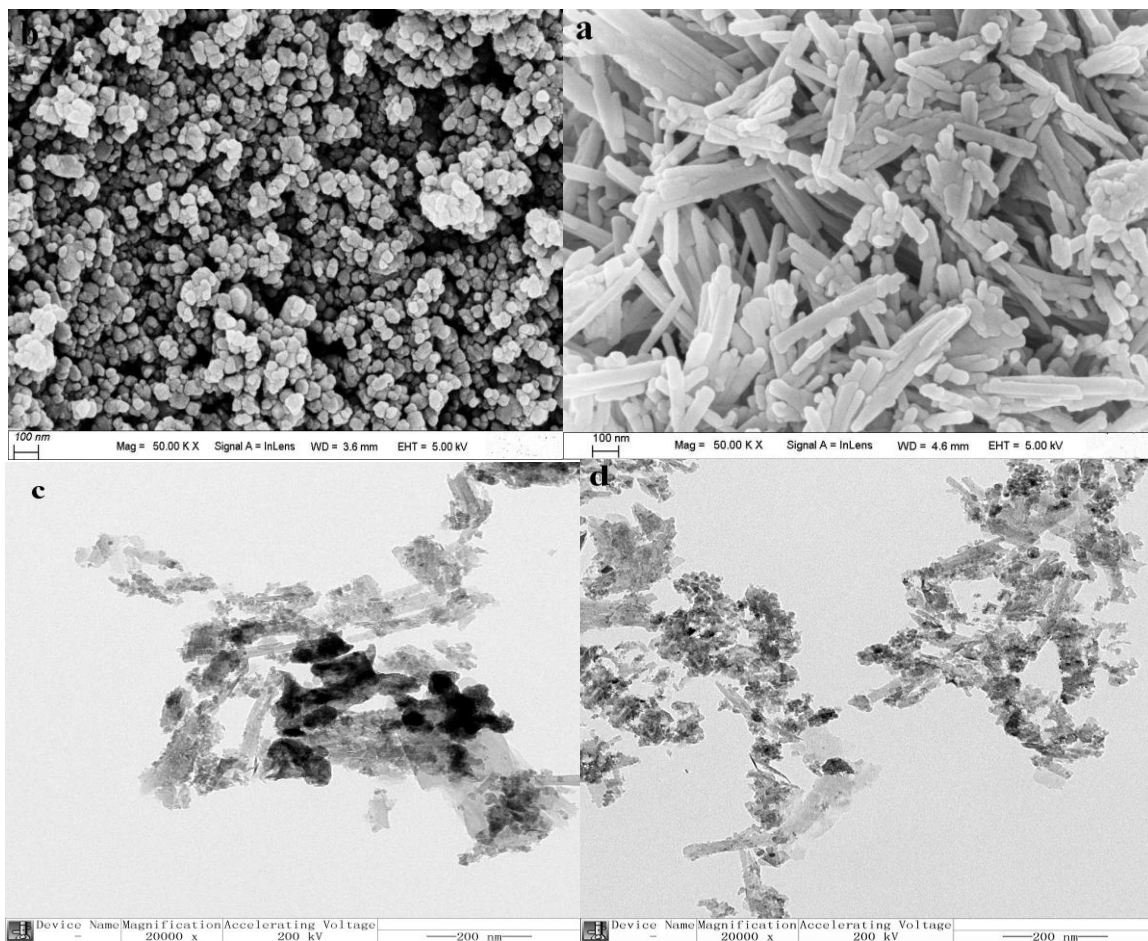


Fig.5: SEM micrographs of carriers (Pal, TiO₂): (a, 100 nm; b, 100 nm), TEM images of untreated and NTP-treated catalysts (c, 200 nm; d, 200 nm).

Characterization and Performance Analysis of NTP-treated Catalysts

Fig.5a, b separately presented the SEM images of the single carrier Pal and TiO₂. Pal showed the long and narrow rod structure, and TiO₂ displayed the spherical particle shape. It could be observed from the TEM images of the untreated and NTP-treated catalysts, as shown in Fig.5c, d, the typical rod structure of Pal for the untreated was not obvious, and there was some black agglomeration over the catalyst, but after treatment, the surface particles were better dispersed, the above reunion phenomenon was vanished.

The acidic sites distributions of the untreated and NTP-treated were determined using NH₃-TPD experiments (Fig.6). No one obvious desorption peaks spanned under the temperature range of 120-500 °C, were seen in the profile of the untreated. Nevertheless, there was respectively one

desorption peak at about 200 °C and 325 °C, which was attributed to the weak acid or strong acid sites, for the NTP-treated catalyst, and it was found that the total amount of the acid sites was higher than that on the untreated. Besides, the surface acidity plays a critical role in the NH₃-SCR system [20].

To obtain more information about the chemical states on the catalyst surface, and to investigate whether the changes of valence band were happened, caused by the NTP treatment, the XPS spectra of Ce 3d and O 1s of the samples were shown in Fig. 7. As could be seen from Fig.7 (A), the Ce 3d XPS spectra of plasma-untreated and plasma-treated samples were assigned to two bands, u and v, respectively; the bands labeled u1 and v1 represented the 3d¹⁰4f¹ initial electronic state, corresponding to Ce³⁺, whereas the rest of bands labeled u, u2, v, v2, u3 and v3 represent the 3d¹⁰4f⁰ state of Ce⁴⁺ ions [19]. The relative ratio of Ce³⁺ (Ce³⁺/ (Ce³⁺ + Ce⁴⁺)) in Ce/TiO₂-Pal (NTP) (34.61 %) was higher than that

of Ce/TiO₂-Pal (22.94 %). This fact indicated that the NTP modification might promoted the reduction from Ce⁴⁺ to Ce³⁺ and thus increased the amount of Ce³⁺, which could induce charge imbalance, more vacancies, and unsaturated chemical bonds, thereby increasing the amount of chemisorbed oxygen[21].

Fig. 7 (B) showed that the O 1s XPS spectra of the above samples, was separated into three types of peaks: the peak at 529.5–530.0 eV labeled O β , at 531.0–531.6 eV labeled O α , and at 532.8–533.0 eV labeled O γ , representing the lattice oxygen O²⁻ (O β), surface chemisorbed oxygen (O α), and defect-oxide or hydroxyl-like group and chemisorbed water (O γ), respectively [22, 23]. Surface chemisorbed oxygen (O α) had been reported to be more active than lattice oxygen because of its higher mobility and it played a significant role in oxidation reactions [24, 25]. Hence, the high O α ratio was of great importance for NO oxidation to NO₂ during the entire SCR reaction. Herein, the higher O α ratio of the treated sample (15.9 %) than that of the untreated one (14.3 %) was related to the higher Ce³⁺ ratio.

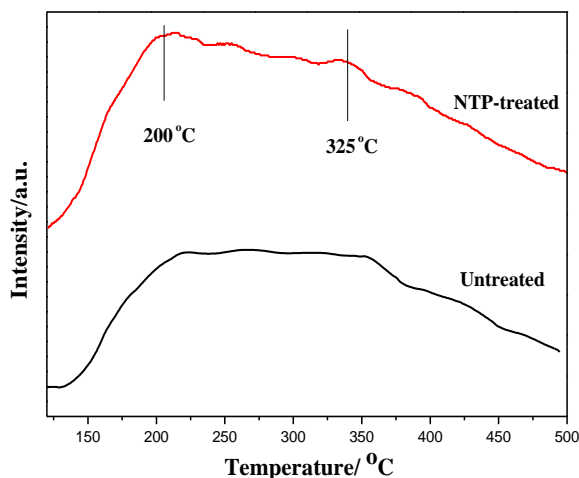
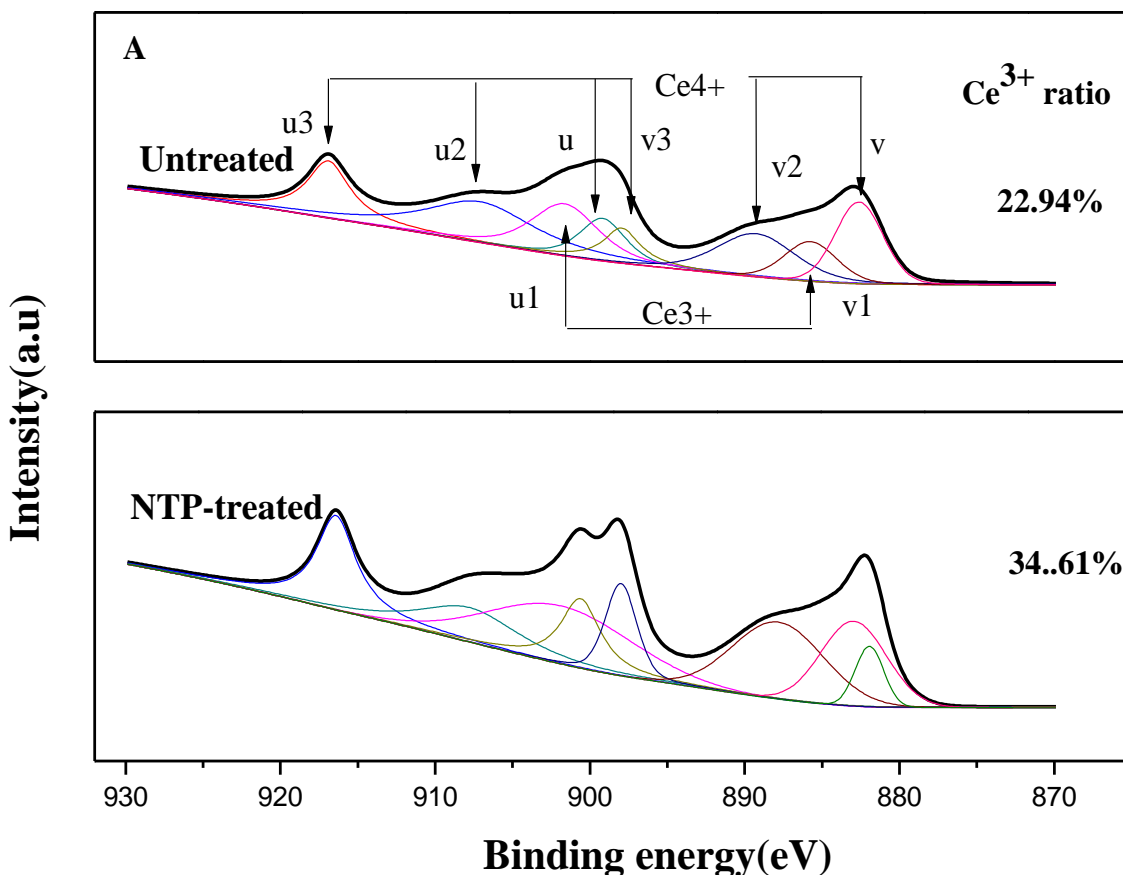


Fig. 6: NH₃-TPD profiles of Ce/TiO₂-Pal (1:3) catalysts (NTP-treated, Untreated).



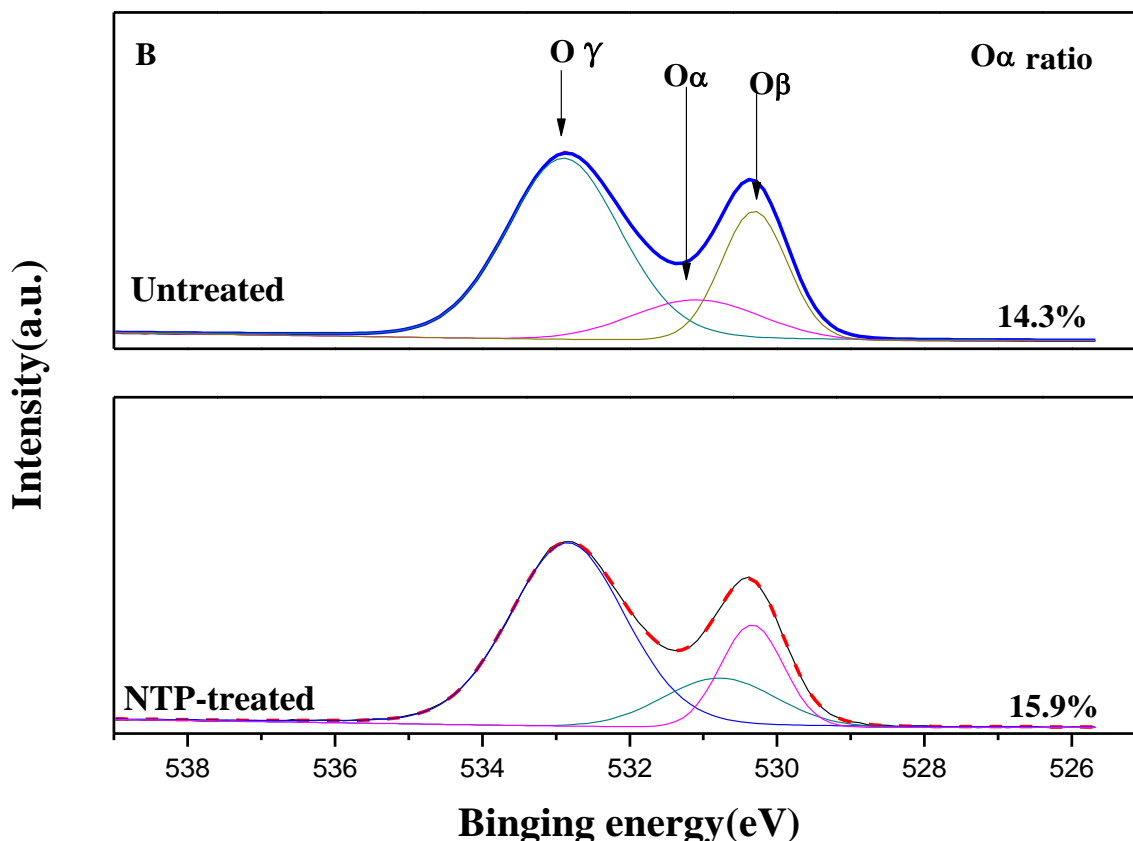


Fig. 7: XPS spectra for (A) Ce 3d and (B) O 1s for Ce/TiO₂-Pal (1:3) catalysts (NTP-treated, Untreated).

To investigate the effect of non-thermal plasma treatment on the NH₃-SCR activity, the catalyst properties, including NO removal efficiency, N₂ selectivity, and alkali resistance, were investigated and the results were illustrated in Figs. 9, 10, and 11. As shown in Fig. 8, the NO conversion efficiency of the sample with NTP modification obviously exceeded that of the catalyst without any changes and became 96.78 % at approximately 350 °C, and it was observed from Fig. 9, the N₂ selectivity of the NTP-treated sample was better than that of the un-pretreated one, which demonstrated that NTP modification could improve the catalytic performance of the Ce/TiO₂-Pal catalyst, due to the improved surface dispersion. In addition, as shown in Fig. 10, doping the plasma-untreated and plasma-treated samples with Na or K, NO conversion efficiency reduced a lot, but better activity was shown in the higher temperature (>400 °C), the K poisoning effect was stronger than Na, and the activity of the NTP-treated was better than that without any treatment. At about 400 °C, the NO conversion of Na-poisoning samples was separately 80.21 %, 83.31 % before and after treatment, and the catalytic activity of K-poisoning samples was 75.26 % and

76.21 %. In general, the plasma treatment could enhance the catalytic performance of the Ce/TiO₂-Pal catalyst, by improving the surface dispersion, leading to the increasing of acid sites, even promoting the transformation from Ce⁴⁺ to Ce³⁺, to result in more surface chemisorbed oxygen.

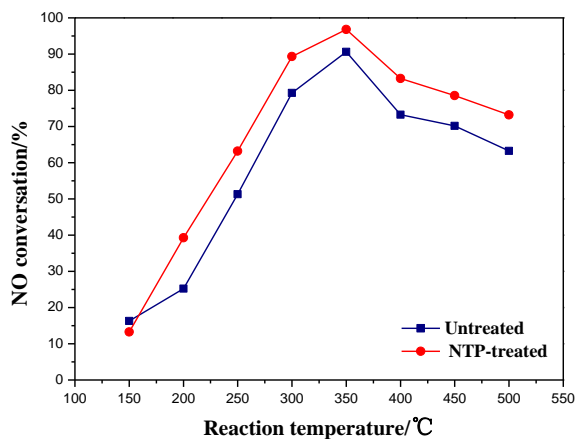


Fig. 8: NO conversion of Ce/TiO₂-Pal (1:3) catalysts (NTP-treated, Untreated).

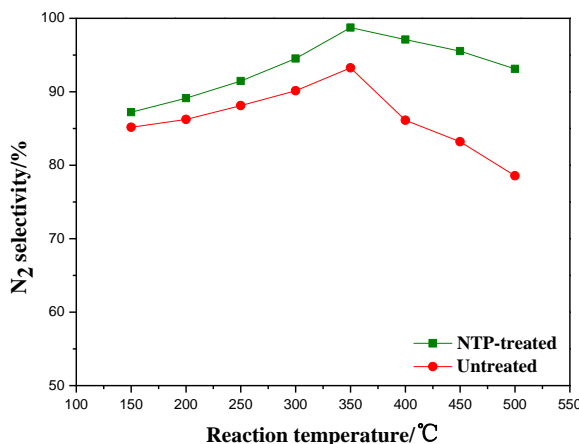


Fig. 9: N₂ selectivity of the Ce/TiO₂-Pal (1:3) catalysts (NTP-treated, Untreated).

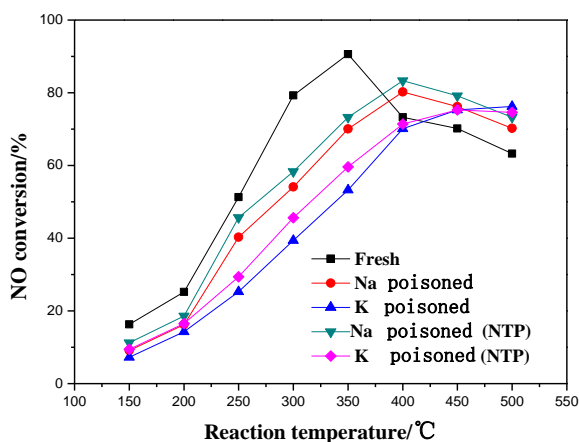


Fig. 10: NO conversion of Ce/TiO₂-Pal (1:3) catalysts (fresh, NTP-poisoning, Untreated-poisoning).

Conclusion

In this work, a series of Ce/TiO₂-Pal catalysts were studied among the NH₃-SCR reaction, in order to further improve the dispersion of the composite catalysts, the plasma was firstly introduced and then calcination was conducted. It could be seen in XPS analysis that the increases in the Ce³⁺ and surface chemisorbed oxygen facilitated the SCR activity of the plasma-treated samples, as a result, the NO conversion efficiency of the untreated and treated, was respectively 90.59 % and 96.78 % at about 350 °C. Furthermore, the N₂ selectivity and alkali resistance was also improved accordingly.

Acknowledgments

This work was financially supported by the national key corpus project development plan

(2016YFC0209203), Qinglan Project, the joint research funds provided by Collaborative Innovation Center for Ecological Building Materials and Environmental Protection Equipment and Key Laboratory for Advanced Technology in Environmental Protection of Jiangsu Province (GX2015106 and GX2015101) and the Science and Technology Project of Jiangsu Province (BY2015057-37, 2016065-36).

References

1. S. Zhang and Q. Zhong, Surface Characterization Studies on the Interaction of V₂O₅-WO₃/TiO₂ Catalyst for Low Temperature SCR of NO with NH₃, *J. Solid State Chem.*, **221**, 49 (2015).
2. S. Roy, M. S. Hegde and G. Madras, Catalysis for NO_x abatement, *Appl. Energy*, **86**, 2283 (2009).
3. H. H. Phil, M. P. Reddy, P. A. Kumar, K. J. Lee and J. S. Hvo, SO₂ resistant antimony promoted V₂O₅/TiO₂ catalyst for NH₃-SCR of NO_x at low temperatures, *Appl. Catal. B- Environ*, **78**, 301 (2008).
4. Q. Li, X. Hou, H. Yang, Z. Ma, J. Zheng, F. Liu, X. Zhang and Z. Yuan, Promotional effect of CeO_x for NO reduction over V₂O₅/TiO₂-carbon nanotube composites, *J. Mol. Catal. A-Chem.*, **356**, 121 (2012).
5. A. S. Negreira and J. Wilcox, DFT Study of Hg Oxidation across Vanadia-Titania SCR Catalyst under Flue Gas Conditions, *J. Phys. Chem. C*, **117**, 1761 (2016).
6. Q. Li, S. Chen, Z. Liu and Q. Liu, Combined effect of KCl and SO₂ on the selective catalytic reduction of NO by NH₃ over V₂O₅/TiO₂ catalyst, *Appl. Catal. B- Environ*, **164**, 475 (2015).
7. E. M. Claesson and A. P. Philipse, Monodisperse magnetizable composite silica spheres with tunable dipolar interactions, *Langmuir*, **21**, 9412 (2009).
8. M. A. L. Vargas, M. Casanova, A. Trovarelli and G. Busca, An IR study of thermally stable V₂O₅-WO₃-TiO₂ SCR catalysts modified with silica and rare-earths (Ce, Tb, Er), *Appl. Catal. B- Environ.*, **75**, 303 (2007).
9. W. Zhao, Y. Tang, Y. Wan and J. Shi, Promotion effects of SiO₂ or/and Al₂O₃ doped CeO₂/TiO₂ catalysts for selective catalytic reduction of NO by NH₃, *J. Hazard. Mater.*, **278**, 350 (2014).
10. Y. Peng, J. Li, L. Chen, J. Chen, J. Han, H. Zhang and W. Han, Alkali metal poisoning of a CeO₂-WO₃ catalyst used in the selective catalytic reduction of NO_x with NH₃: an experimental and

- theoretical study, *Environ. Sci. Technol.*, **46**, 2864 (2017).
11. W. Cha, S. Chin, E. Park, S. Yun and J. Jurng, Effect of V₂O₅ loading of V₂O₅/TiO₂ catalysts prepared via CVC and impregnation methods on NO_x removal, *Appl. Catal. B- Environ.*, **140**, 708 (2013).
 12. A. Łamacz, A. Krztoń and G. Djéga-Mariadassou, Study on the selective catalytic reduction of NO with toluene over CuO/CeZrO₂. A confirmation for the three-function model of HC-SCR using the temperature programmed methods and in situ DRIFTS, *Appl. Catal. B- Environ.*, **142**, 268 (2013).
 13. F. Liu, H. He, Z. Lian, Z. Shan, W. Xie, K. Asakura, W. Yang and H. Deng, Highly dispersed iron vanadate catalyst supported on TiO₂ for the selective catalytic reduction of NO_x with NH₃, *J. Catal.*, **307**, 340 (2013).
 14. C. J. Liu, K. Yu, Y. P. Zhang, X. L. Zhu and F. He, Characterization of Plasma Treated Pd/HZSM-5 Catalyst for Methane Combustion, *Appl. Catal. B- Environ.*, **47**, 95 (2004).
 15. Q. R. Li, J. B. Wu and J. M. Hao, NO_x Storage Capacity Enhancement on NiO/Al₂O₃ Pretreated with a Non-thermal Plasma, *Chin. J. Catal.*, **32**, 572 (2011).
 16. X. Tang, F. Gao, Y. Xiang, H. H. Yi and S. Z. Zhao, Low Temperature Catalytic Oxidation of Nitric Oxide over the Mn-CoO_x Catalyst Modified by Non-thermal Plasma, *Catal. Commun.*, **64**, 12 (2015).
 17. F. Xiao, Y. J. Gu, Z. Tang, F. V. Han and Q. Xu, Selective Catalytic Reduction of NO with NH₃ on Stannic and Iron Bimetal Oxides/Attapulgite Catalysts, *J. Chem. Pharm. Res.*, **6**, 281 (2014).
 18. K. Cheng, J. Liu, T. Zhang, J. M. Li, Z. Zhao, Y. C. Wei, G. Y. Jiang and A. J. Xie, Effect of Ce Doping of TiO₂ Support on NH₃-SCR Activity over V₂O₅-WO₃/CeO₂-TiO₂ Catalyst, *J. Environ. Sci.*, **26**, 2106 (2014).
 19. L. Chen, J. Li and M. Ge, Promotional Effect of Ce-doped V₂O₅-WO₃/TiO₂ with Low Vanadium Loadings for Selective Catalytic Reduction of NO_x by NH₃, *J. Phys. Chem. C*, **113**, 21177 (2009).
 20. Y. Peng, R. Qu, X. Zhang and J. Li, The relationship between structure and activity of MoO₃-CeO₂ catalysts for NO removal: influences of acidity and reducibility, *Chem. Commun.*, **49**, 6215 (2013).
 21. H. Li, C. Y. Wu, Y. Li and J. Zhang, Superior Activity of MnO_x-CeO₂/TiO₂ Catalyst for Catalytic Oxidation of Elemental Mercury at Low Flue Gas Temperatures, *Appl. Catal. B: Environ.*, **111**, 381 (2012).
 22. J. C. Dupin, D. Gonbeau and P. Vinatier, Systematic XPS Studies of Metal Oxides Hydroxides and Peroxides, *Phys. Chem. Chem. Phys.*, **2**, 1319 (2000).
 23. J. Fang, X. Bi, D. Si, Z. Jiang and W. Huang, Spectroscopic Studies of Interfacial Structures of CeO₂-TiO₂ Mixed Oxides, *Appl. Surf. Sci.*, **2253**, 8952 (2007).
 24. T. Gu, Y. Liu, X. Weng, H. Wang and Z. Wu, The Enhanced Performance of Ceria with Surface Sulfation for Selective Catalytic Reduction of NO by NH₃, *Catal. Commun.*, **12**, 310 (2010).
 25. M. Kang, E. D. Park, M. K. Ji and J. E. Yie, Manganese Oxide Catalysts for NO_x Reduction with NH₃ at Low Temperatures, *Appl. Catal. A: Gen.*, **327**, 261 (2007).